Apparent Temperature Dependence on Localized Atmospheric Water Vapor

Matthew Montanaro[a], Carl Salvaggio[a], Scott D. Brown[a], David W. Messinger[a], and Alfred J. Garrett[b]

[a]Rochester Institute of Technology, 54 Lomb Memorial Drive, Rochester, NY, USA;
[b]Savannah River National Laboratory, Building 735-A, Office B108, Aiken, SC, USA

ABSTRACT

The atmosphere is a critical factor in remote sensing. Radiance from a target must pass through the air column to reach the sensor. The atmosphere alters the radiance reaching the sensor by attenuating the radiance from the target via scattering and absorption and by introducing an upwelling radiance. In the thermal infrared, these effects will introduce errors in the derived apparent temperature of the target if not properly accounted for. The temperature error is defined as the difference between the target leaving apparent temperature and observed apparent temperature. The effects of the atmosphere must be understood in order to develop methods to compensate for this error. Different atmospheric components will affect the radiation passing through it in different ways. Certain components may be more important than others depending on the remote sensing application. The authors are interested in determining the actual temperature of the superstructure that composes a mechanical draft cooling tower (MDCT), hence water vapor is the primary constituent of concern. The tower generates a localized water vapor plume located between the target and sensor. The MODTRAN radiative transfer code is used to model the effects of a localized exhaust plume from a MDCT in the longwave infrared. The air temperature and dew point depression of the plume and the thickness of the plume are varied to observe the effect on the apparent temperature error. In addition, the general atmospheric conditions are varied between two standard MODTRAN atmospheres to study any effect that ambient conditions have on the apparent temperature error. The Digital Imaging and Remote Sensing Image Generation (DIRSIG) modeling tool is used to simulate the radiance reaching a thermal sensor from a target after passing through the water vapor plume. The DIRSIG results are validated against the MODTRAN results. This study shows that temperature errors of as much as one Kelvin can be attributed to the presence of a localized water vapor plume.

Keywords: MODTRAN, RADIANCE PROPAGATION, APPARENT TEMPERATURE, THERMAL INFRARED, SYNTHETIC IMAGE GENERATION

1. INTRODUCTION

The derivation of the absolute temperature of a material from remotely sensed imagery is a difficult problem. The radiance reaching a sensor from a target material is dependent on the emissivity and geometry of the material and on the intervening atmosphere [1]. The emissivity and angular effects can be neglected if the target material is assumed to be a perfect blackbody. The atmospheric effects must then be accounted for in order to translate the apparent temperature recorded by the sensor into the absolute temperature of the target. There are many methods presented in the literature that account for these atmospheric effects [1]. Temperature estimation from measurements in a broadband 8 - 14 μm infrared window were used in this study. This method requires knowledge of the temperature and water vapor profile in the air column between the target and sensor. Water vapor absorption and emission dominates the 8 - 14 μm longwave infrared (LWIR) region [2].

The MODerate spectral resolution TRANsmittance radiative transfer model was used to model how the water vapor concentration affects the target-to-sensor transmission and upwelled radiance in the atmosphere at longwave infrared wavelengths [3]. Two atmospheric layers were defined in MODTRAN. The first layer extended from the ground to a specified height. This layer was representative of the exhausted water vapor plume from a

Send correspondence to Matthew Montanaro: E-mail: mxm9876@cis.rit.edu

Algorithms and Technologies for Multispectral, Hyperspectral, and Ultraspectral Imagery XIV, edited by Sylvia S. Shen, Paul E. Lewis, Proc. of SPIE Vol. 6966, 696618, (2008) · 0277-786X/08/$18 · doi: 10.1117/12.774694

mechanical draft cooling tower. The second layer extends from the first (plume) layer up to an observation altitude of one hundred meters. This layout is illustrated in Figure 2. The air temperature and dew point depression in the plume layer and the thickness of the plume were varied to observe the effect on the total transmission and upwelling radiance in the air column between the sensor and target. In addition, the general atmospheric conditions were varied between two standard MODTRAN atmospheres to study any effect of ambient conditions on the transmission. The target temperature was also varied to determine its effect on the derived apparent temperature. MODTRAN calculates the spectral transmissions and spectral upwelled radiances for each set of atmospheric parameters that were varied. These spectral values along with the Planck equation were used to convert the radiance reaching a thermal infrared sensor from a blackbody into an estimate of the apparent temperature of the blackbody. A temperature error was then defined as the difference between the actual temperature of the blackbody and the atmosphere-affected estimated temperature. The results demonstrate that the temperature errors increase as the water vapor concentration increases. The target's blackbody temperature also has a profound impact on the temperature errors.

A similar situation was created in the Digital Imaging and Remote Sensing Image Generation (DIRSIG) modeling tool. A longwave infrared sensor was placed 100 meters above a blackbody plate. A localized water vapor plume was placed above the blackbody. The thickness of the plume and the ambient atmospheric conditions were consistent with the MODTRAN simulations. A temperature error was similarly defined as the difference between the actual temperature of the blackbody plate and the apparent temperature recorded by the sensor. The DIRSIG results were then compared to the MODTRAN results.

2. BACKGROUND

Radiance from a blackbody material may be heavily modified as it propagates through the atmosphere to reach an overhead nadir-looking sensor. The blackbody radiance as described by the Planck equation is both attenuated and exaggerated by the atmospheric constituents.

2.1 Blackbody Radiance

The radiance emitted from an ideal blackbody material is dependent on the temperature of the material and is described by the Planck equation as,

$$L_{BB}(\lambda, T) = \frac{2hc^2}{\lambda^5}\left[e^{\frac{hc}{\lambda kT}} - 1\right]^{-1} \qquad \left[\frac{W}{m^2\ sr\ \mu m}\right], \tag{1}$$

where h is Planck's constant $\left(6.6256 \cdot 10^{-34}\ [J \cdot s]\right)$, c is the speed of light in vacuum $\left(2.9979 \cdot 10^{8}\ [m/s]\right)$, k is Boltzmann's constant $\left(1.3807 \cdot 10^{-23}\ [J/K]\right)$, T is the absolute temperature of the material, and λ is the wavelength of the radiation.

2.2 Atmospheric Effects

The radiance leaving a blackbody material must propagate through the atmosphere to reach the sensor. The atmosphere may considerably modify this radiance along the line of sight to the sensor. The constituent gases and aerosols attenuate the signal by absorption and scattering of photons. This phenomenon is captured by the atmospheric transmission parameter, $\tau(\lambda)$. The atmospheric constituents also have a finite temperature and will emit their own radiance in all directions, thereby adding to the apparent material radiance [4]. This radiance from the air column between the target and sensor is known as the path radiance, or upwelled radiance, $L_u(\lambda)$. A similar downwelled term is ignored here as the materials being considered have zero reflectance.

2.2.1 Atmospheric Transmission

Atmospheric transmission encompasses both the absorption and scattering of photons. Absorption refers to the removal of photons by a material through the conversion of electromagnetic energy to some other form of energy, usually thermal. It occurs when the energy (wavelength) of the incoming photon is sufficient to cause a rotational, vibrational, or electronic energy transition. The molecule absorbs the photon and makes a quantum jump to a higher energy state. The molecule will quickly lose this excess energy through collisions with other

molecules and return to its original energy state. The photon energies (wavelengths) that will be absorbed by a molecule depend on the transition energies between states of that molecule [5]. The amount of absorption by atmospheric gases is dependent on the quanitity of the gas and on its temperature and pressure [4]. Major absorbers in Earth's atmosphere in the longwave infrared are O_3, CO_2, and H_2O.

Transmission losses are also the result of photons being scattered out of the propagating beam. Ordinary gas molecules in the atmosphere do not produce significant scattering in the longwave infrared [6][7]. Scattering will become important in the LWIR if dust particles and aerosols are present in the atmosphere.

2.2.2 Atmospheric Emission

The constituents of the atmosphere have a finite temperature and will therefore be a source of radiance. Part of this radiance is emitted towards the target material and is known as the emissive downwelled radiance, $L_d(\lambda)$. Some of the atmospheric thermal energy is emitted towards the sensor and is known as the emissive upwelled radiance, $L_u(\lambda)$. The upwelled radiance and the reflected downwelled radiance add to the target material's signal as recorded by the sensor [6].

2.3 Radiance Reaching the Sensor

The total spectral radiance reaching the sensor from a blackbody target is then

$$L_{sensor}(\theta, \phi, \lambda) = \tau(\theta, \phi, \lambda)\, L_{BB}(\lambda, T) + L_u(\theta, \phi, \lambda) \qquad \left[\frac{W}{m^2\, sr\, \mu m}\right] \tag{2}$$

where (θ, ϕ) indicate the direction of the sensor. This equation represents the radiance reaching the front of the sensor from a blackbody material after passing through the air column.

2.4 Effective Radiance and Apparent Temperature

A sensor is only responsive to a certain range of wavelengths known as its bandpass. The responsivity of the sensor to each wavelength is represented by the spectral response function, $R'(\lambda)$, which is a combined effect of the optics and the wavelength sensitivity of the detector. It is a unitless value between zero and unity describing the fraction of radiation that is recorded by the sensor at a particular wavelength. A typical broadband infrared sensor might have a response close to unity in the 8 - 14 μm region and a zero response outside that region.

The sensor-reaching radiance is weighted by the response function and integrated over all wavelengths (essentially the bandpass of the sensor) to produce an effective integrated radiance [6]. Mathematically, this effective magnitude of the sensor-reaching radiance relative to the spectral response of the sensor is stated as

$$L_{eff} = \int_0^\infty L_{sensor}(\theta, \phi, \lambda)\, R'(\lambda)\, d\lambda \qquad \left[\frac{W}{m^2\, sr}\right]. \tag{3}$$

This integrated radiance reported by the sensor may be converted into an apparent temperature. The Planck formula produces a spectral radiance for a given temperature and wavelength. To incorporate the spectral nature of the blackbody radiance and the spectral response of the sensor, a look-up table (LUT) can be generated to accurately convert the sensor's integrated radiance into an apparent temperature [8]. The apparent temperature may then be compared to the actual temperature of the blackbody material.

3. MODTRAN SIMULATION OF MDCT EXHAUST PLUME

A MDCT ultilizes evaporative processes. Therefore the exhaust plume consists of water vapor at an elevated temperature into the volume immediately above the tower. Radiance emitted within the tower must pass through this plume to reach an airborne sensor. The air column can be divided into two segments. The first segment falls within the exhaust plume of the tower. The second segment is the free atmosphere not influenced by the plume. Figure 1 demonstrates radiance from the tower passing through the exhaust plume to reach the sensor.

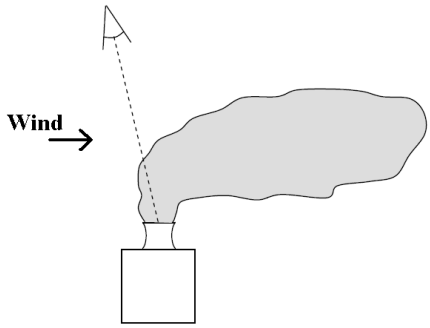

Figure 1. Radiance from the tower passes through the exhaust plume to reach the sensor.

Transmission values of less than unity will decrease the radiance at the sensor resulting in an apparent temperature that is lower than the actual material temperature. Conversely, the upwelled radiance will increase the radiance at the sensor resulting in an apparent temperature that is higher than the actual material temperature. These two effects compete with each other so that the apparent temperature at the sensor may be higher or lower than the actual temperature depending on the state of the atmosphere. The state of the atmosphere must be carefully modeled in order to correct for errors in the derived temperature.

The first segment, representing the plume, would contain a higher water vapor concentration than the second segment (in most cases) and would therefore be more influencial in the transmission and upwelled factors. The free parameters of the plume affecting these factors are the air temperature, the moisture content, and the height. The ambient atmospheric conditions (second segment) will also affect the transmission and upwelled separately. The MODTRAN tool can be used to model the effect of the air column on the derived apparent temperature at the sensor.

3.1 Simulation Approach

The MODTRAN radiative transfer model was used to model how the water vapor concentration affects the transmission and upwelled radiance in the atmosphere in the longwave infrared region. The dew point depression and air temperature were chosen as measures of the water vapor concentration in the column due to their feasibility of measurement in situ. The air column was divided into two layers in MODTRAN. The first layer extends from the ground to a height of z meters to represent the exhausted plume. The second layer extends from the terminating point of the first layer up to an observation altitude of 100 meters. The second layer was assigned standard atmospheric conditions. The first layer was also assigned standard conditions for all parameters except the air temperature and the dew point depression which were varied. Figure 2 illustrates this layout.

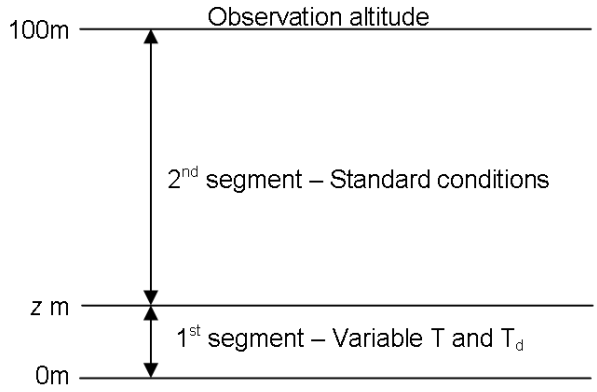

Figure 2. Atmospheric conditions modeled in MODTRAN.

Several MODTRAN runs were conducted under a variety of conditions. The air temperature in the first layer was varied in increments of 5 K from 280 K to 310 K. For each temperature, dew point depressions of 0, 2, 5, 10, and 20 K were used. The dew point depression is the difference between the air temperature and the dew point temperature. A dew point depression close to zero indicates near saturated air while a large depression indicates dryer air. The observation altitude was held fixed at 100 m. The thickness of the first layer, z, was set to values of 1, 5, 10, and 20 m representing various plume thicknesses under a variety of ambient wind conditions (i.e. - lower wind speed indicates a more vertical plume and a thicker layer). The above parameters were run for standard mid-latitude summer conditions and then repeated for sub-arctic winter conditions representing relatively wet and dry ambient atmospheres, respectively. The target material was a perfect blackbody. Several runs were performed with blackbody targets of 302 K, 306 K, and 310 K. MODTRAN4v3r1 was run in solar/thermal radiance mode between 8 and 14 μm at a resolution of 0.3 μm with an 8-stream discrete ordinate multiple scattering algorithm [9].

The intent of the MODTRAN simulation was to model an air column containing a high water vapor concentration layer within a column of standard water vapor conditions. The transition between this lower layer and the standard atmosphere is marked by a dramatic gradient in the water vapor profile. In a user defined atmosphere, MODTRAN allows the user to specify the height, pressure, temperature and dew point of the atmospheric layer at each altitude. These supplied values are used at the exact heights specified. However, MODTRAN's interpolation scheme is inadequate for such large gradients across large, relatively broad altitude ranges [10]. Therefore, in order to realize the strength of this gradient, several thinner (one meter thick) layers were inserted between the standard layers of the upper atmosphere and the user-defined, high humidity conditions of the lowest layer. These extra layers provided the necessary buffer to allow a sharp fall off in temperature and dew point depression between the first and second layers. Figure 3 demonstrates the layers set in MODTRAN.

The modified parameters for the MODTRAN simulations were the height of the plume segment, the air temperature and dew point depression in the plume, and the ambient atmospheric conditions. Table 1 summarizes these parameter values. A MODTRAN run was performed for every combination. The model output contains

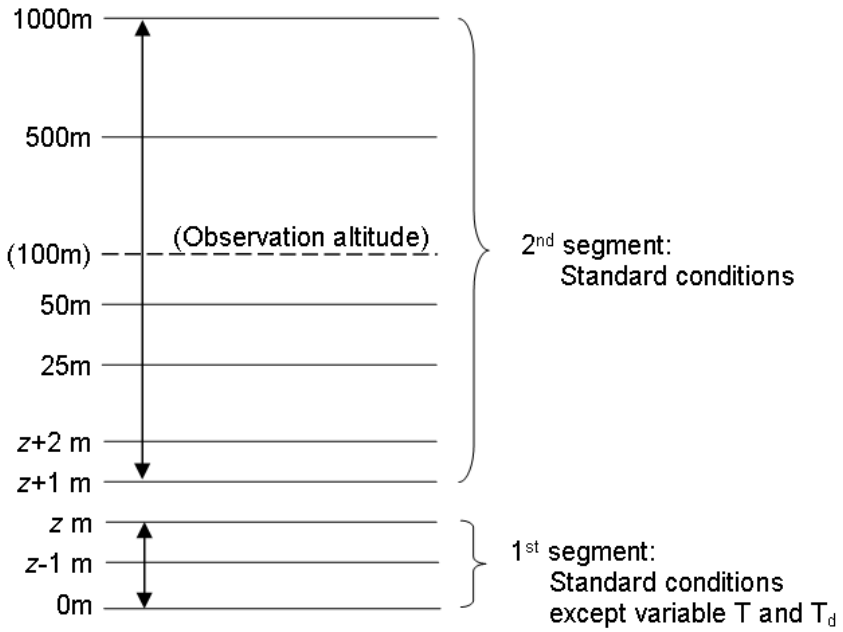

Figure 3. Schematic of the atmospheric layers assigned in MODTRAN. The first segment represents the exhaust plume while the second segment represents the rest of the air column. Standard atmospheric conditions are assigned to every layer except for those in the first segment where the air temperature and dew point temperature are varied (not to scale).

spectral values of the transmission (TRANS) and upwelled radiance (PATH_THERMAL) between wavelengths of 8 and 14 μm. These spectral values were used to calculate the radiance reaching a sensor from several blackbody targets through equation (2). The material radiance was taken as the spectral blackbody radiance from the Planck equation. Temperatures of 302 K, 306 K, and 310 K were used for the targets. The spectral radiance at the sensor from equation (2) was integrated between 8 and 14 μm to arrive at an integrated radiance at the sensor. The simulated sensor had a flat, unit spectral response function between 8 and 14 μm and a zero response outside that region. The integrated sensor radiance was converted to an apparent temperature via a look-up table. Finally, the temperature error was defined as the difference between the blackbody temperature used in the Planck equation and the apparent temperature derived from the integrated sensor radiance,

$$T_{error} = T_{BB} - T_{App} \qquad [K]\,. \tag{4}$$

Blackbody Temp. [K]	**Plume Height [m]**	**Plume Air Temp. [K]**	**Plume Dew Pt. Depression [K]**	**Ambient Conditions**
302	1	280	0	mid-latitude summer
306	5	285	2	sub-arctic winter
310	10	290	5	
	20	295	10	
		300	20	
		305		
		310		

Table 1. Parameter values for the MODTRAN simulations

3.2 Simulation Results

The results of the simulations are shown in Figures 4 and 5. By visual inspection, the material blackbody temperature has the greatest influence on the temperature error, followed by the ambient atmospheric conditions, and then the plume. In general, the target blackbody temperature and the ambient atmospheric conditions affect the overall magnitude of the temperature errors (magnitude of the surfaces in Figures 4 and 5) and the plume influences the shape of the surface.

The material kinetic temperature influences the temperature errors. A greater kinetic temperature for the material results in a higher temperature error. The reason for this trend is apparent in equations (2) and (4). The temperature error is proportional to the difference between the material blackbody radiance and the sensor-reaching radiance such that,

$$\begin{aligned} T_{error} &\propto L_{BB} - L_{sensor} \\ &\propto L_{BB} - (\tau\, L_{BB} + L_u) \\ &\propto (1-\tau)\, L_{BB} - L_u. \end{aligned} \tag{5}$$

A higher blackbody temperature, L_{BB}, would result in a higher radiance. Although the transmission does not change as the blackbody temperature changes, the result of the blackbody radiance multiplied by the transmission is greater for high target temperatures than for low temperatures. The first term is larger for a higher blackbody radiance than for a lower blackbody radiance. The sensor radiance will therefore also be higher as will the resulting temperature errors.

The effect of the plume becomes apparent as the plume thickness increases, thus increasing the integrated water vapor along the path. There is a competing effect of transmission losses and additive upwelled radiance.

Mid-Latitude Summer Conditions

Atmospheric Conditions at $z = 25m$: $P = 1010.065mb$, $T = 294.09K$, $Dew\,Pt.\,Depress. = 4.41K$

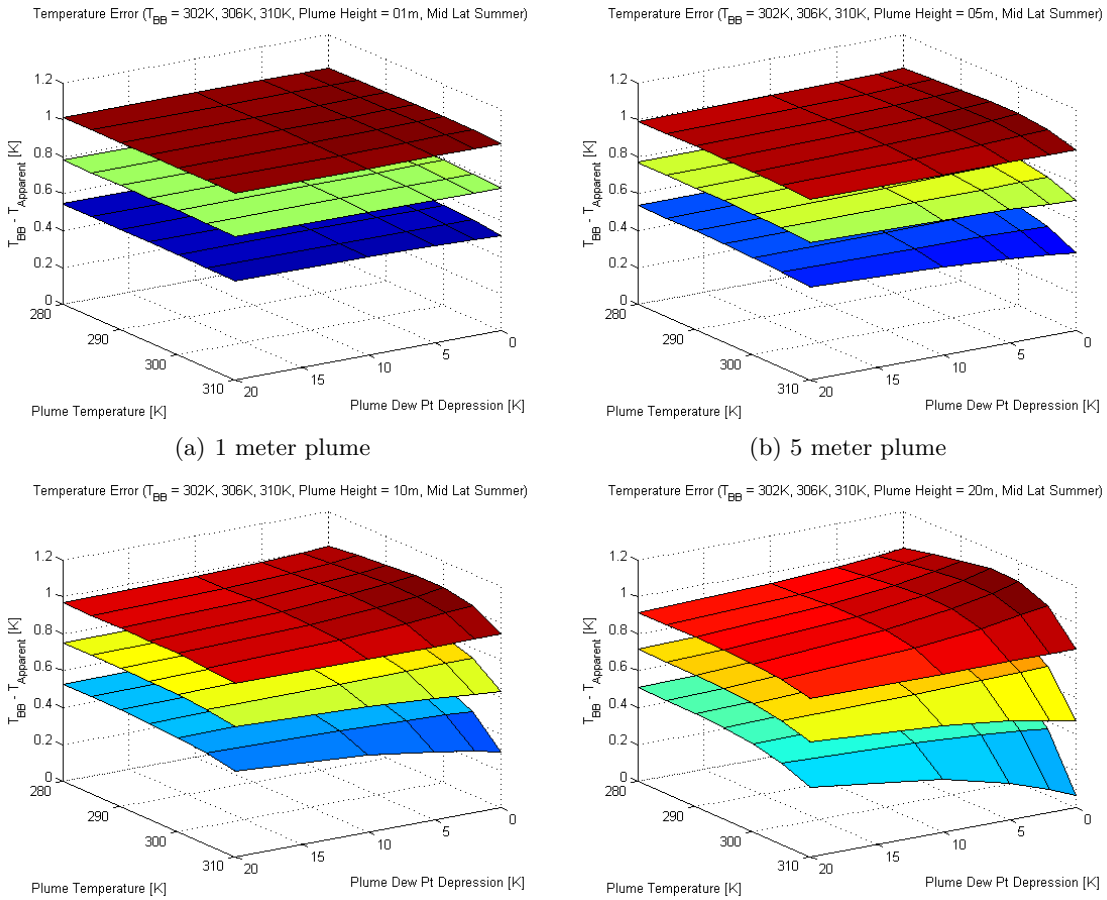

(a) 1 meter plume

(b) 5 meter plume

(c) 10 meter plume

(d) 20 meter plume

Figure 4. Errors between material blackbody temperature and the sensor derived apparent temperature. The surfaces are for material blackbody temperatures of 310 K, 306 K, and 302 K from top to bottom in each plot.

Sub-Arctic Winter Conditions

Atmospheric Conditions at $z = 25m$: $P = 1009.664mb$, $T = 257.25K$, $Dew\,Pt.\,Depress. = 2.36K$

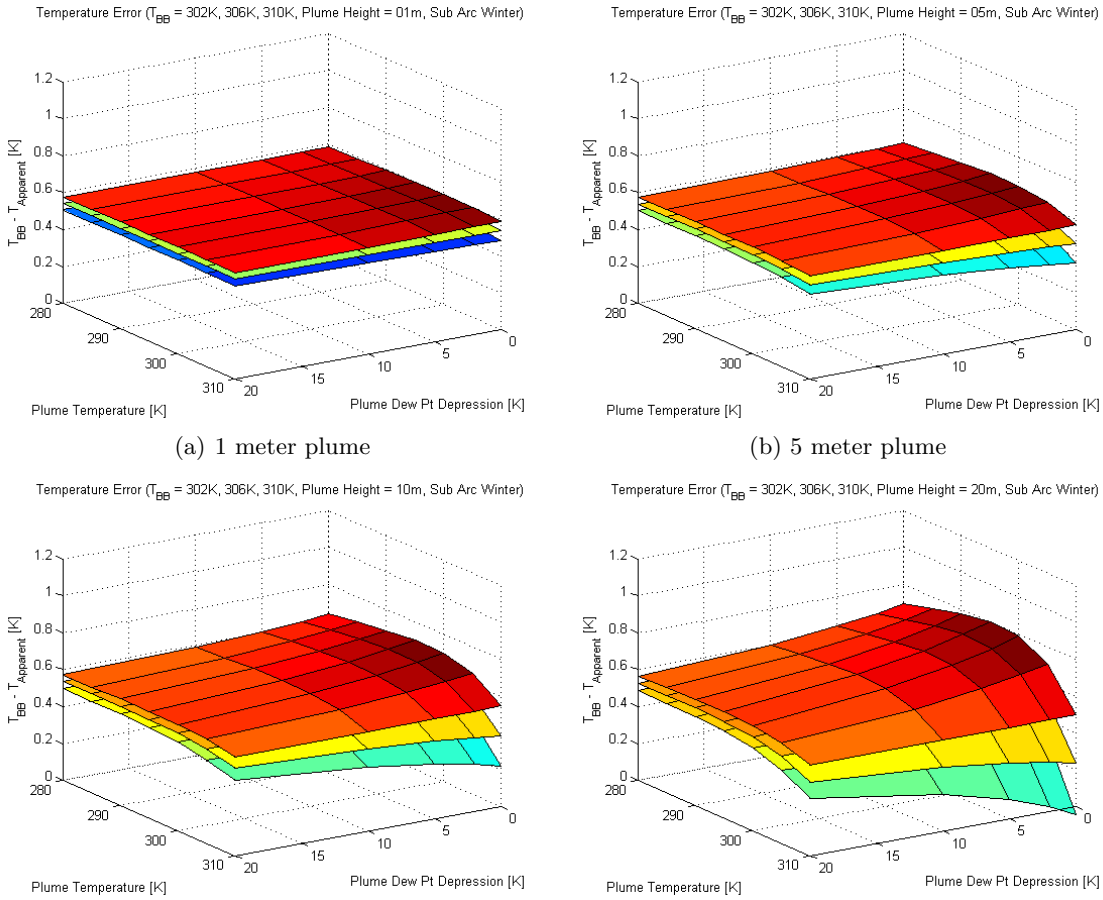

(a) 1 meter plume

(b) 5 meter plume

(c) 10 meter plume

(d) 20 meter plume

Figure 5. Errors between material blackbody temperature and the sensor derived apparent temperature. The surfaces are for material blackbody temperatures of 310 K, 306 K, and 302 K from top to bottom in each plot.

The temperature error seems to peak for a plume temperature of 295 K to 300 K at a dew point depression of 0 K (saturated). The minimum temperature error occurs for the highest set plume temperature of 310 K and a dew point depression of 0 K. The range of temperature errors increase as the plume thickness increases.

Finally the overall temperature errors are greater under mid-latitude summer conditions than for sub-arctic winter conditions. A mid-latitude summer atmosphere is warmer and contains a greater amount of water vapor which leads to a decreased transmission and increased upwelled radiance. However, the transmission loss has a greater effect than the upwelled radiance in this case which results in increased temperature errors. Conversely, a sub-arctic winter atmosphere is much drier and colder. The transmission values are higher and the upwelled radiance is less for this atmosphere. The combined effect is a lower temperature error.

There is a peculiar data value in Figure 5(d) that is worth noting. The temperature error becomes negative for a blackbody target of 302 K, a plume temperature of 310 K and a dew point depression of zero. An error of less than zero implies that the image-derived apparent temperature is greater than the actual material blackbody temperature. In this case, the upwelled radiance dominates over the transmission loss which results in a higher radiance at the sensor. A plot of the target's blackbody radiance modified by the spectral transmission and the spectral upwelling radiance is shown in Figure 6. For reference, a blackbody curve at 302 K is also shown. The curves seem to show that the transmission loss is at least compensated for by the upwelled radiance.

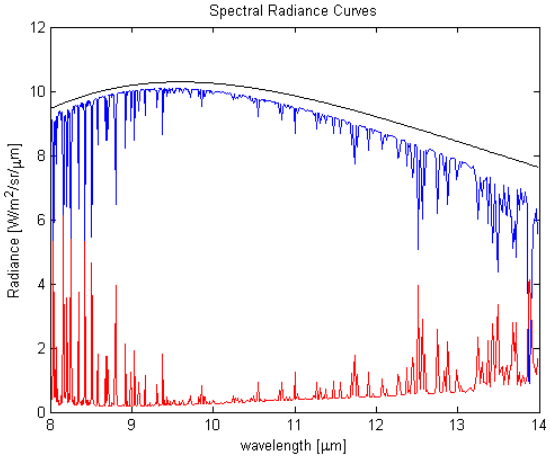

Figure 6. Comparison of the radiometric terms for the 310 K plume temperature and 0 K dew point depression from Figure 5d. Blackbody spectrum for 302 K (top), blackbody spectrum modified by the spectral transmission (middle), and the spectral upwelled radiance (bottom).

4. WATER VAPOR PLUME IN DIRSIG

The MODTRAN study of the localized water vapor plume was extended into a synthetic three dimensional physical model in the DIRSIG modeling environment [11]. The DIRSIG model is intended to replicate the MODTRAN simulation of the apparent temperature dependence on a localized water vapor plume and on the ambient atmospheric conditions. The radiometric accuracy of the DIRSIG model is validated against the MODTRAN results. A combination of MODTRAN parameters listed in Table 1 was chosen to be reproduced in DIRSIG. The intent was to investigate whether a similar temperature error is predicted under the same conditions.

The plume model implemented in DIRSIG is based on the Monte Carlo smoke plume model described by Blackadar [12]. A DIRSIG rendering of a plume over a MDCT is shown in Figure 7. The Blackadar plume model requires the concentration and a spectral extinction curve for the water vapor plume. These parameters may be derived from the MODTRAN output. A particular plume temperature, dew point depression, plume height, and ambient conditions from the previous MODTRAN runs were chosen. The amount of additional water vapor

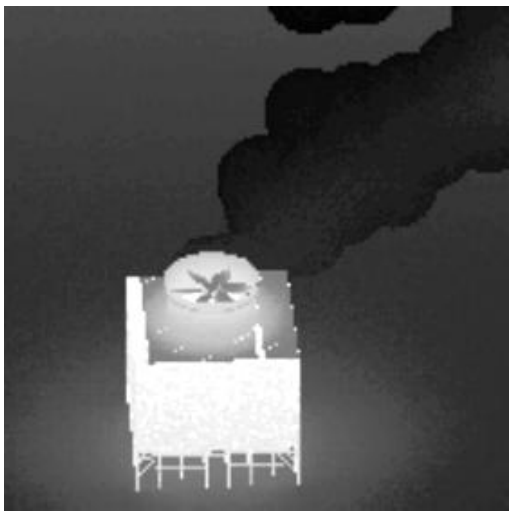

Figure 7. DIRSIG rendering of a MDCT and its water vapor plume in the LWIR.

introduced by the plume must be determined. The MODTRAN input data file for this condition was modified so that the sensor altitude was the same as the height of the plume. In other words, the air column between the target and the sensor (H2 and H1) consisted of the plume layer only. MODTRAN is run in Solar/Thermal Radiance mode and the amount of water vapor under the TOTAL COLUMN ABSORBER AMOUNTS FOR THE LINE-OF-SIGHT PATH section is recorded. The units are ATM-CM and must be converted to parts-per-million (ppm) in order to be used in DIRSIG. This number is the total amount of water vapor in the plume layer. To get only the *additional* water vapor that was added by the plume, the same MODTRAN input data file is modified so that the water vapor and air temperature in the plume layer is set to the default values for the given ambient conditions. The column absorber amount for water vapor is again taken from the MODTRAN output and converted to ppm. The difference between the two column absorber amounts (with and without the elevated water vapor) is the amount of additional water vapor introduced by the plume.

DIRSIG also requires a spectral extinction curve for water vapor in addition to the concentration. The extinction curve for the additional water vapor introduced by the plume can be derived from the MODTRAN output in the same way as described above. The same MODTRAN input file as before (with the elevated water vapor) is modified to run in transmittance mode. The water extinction is due to both molecular and continuum absorption. The water vapor and water continuum transmission columns in the MODTRAN output are multiplied together to get the total water vapor transmission curve. This transmission curve is then converted into an extinction curve in units of $\frac{1}{ppm-m}$. As before, the extinction due to the *additional* water vapor is needed. The MODTRAN input file is amended so that the water vapor in the plume is set to the default ambient conditions. The water vapor and water continuum transmission columns in the MODTRAN output are multiplied together and converted to an extinction curve. Finally, the extinction curve due to only the additional water vapor is found by subtracting the two previously calculated extinction curves.

A DIRSIG scene was constructed that consisted of a blackbody plate set to a temperature of 306 K. A longwave infrared sensor with a unit response between 8 and 14 μm and zero elsewhere was positioned 100 meters directly above the blackbody plate (as in the MODTRAN runs). The DIRSIG Blackadar plume model requires the temperature of the plume and the concentration and spectral extinction for the constituent gas of the plume. The concentration and extinction were derived from MODTRAN as described above. To mimic the height of the plume layer in MODTRAN, the DIRSIG plume can be set to only a single "puff" of water vapor at a specified diameter. The diameter of this puff is then set to the height of the MODTRAN plume layer and the concentration and extinction of the puff is set to the MODTRAN derived values. The temperature of the puff and the ambient atmospheric conditions were also set to the same values that were used in the MODTRAN simulation. The radiance recorded by the sensor is then converted into an apparent temperature.

The atmospheric parameters from the MODTRAN runs that were repeated in the DIRSIG simulation are a plume height of 10 meters, plume temperature and dew point depression of 305 K and 5 K, under mid-latitude summer conditions. The material blackbody temperature is 306 K. The resulting apparent temperature error in DIRSIG is 0.724 K. The same parameters in MODTRAN yielded a temperature error of 0.737 K. The DIRSIG predicted error is within 1.8 % of the MODTRAN predicted error.

5. CONCLUSIONS

The result of this analysis reveals that knowledge of the water vapor content in the target-to-sensor path is very important to accurately derive the temperature of the MDCT. There is a competing effect of transmission loss and additive upwelled radiance. In general, the temperature errors are higher for a thicker plume and when the ambient conditions are warmer and more moist. The target material's blackbody temperature also affects the temperature errors such that a higher blackbody temperature results in a higher temperature error.

The MODTRAN simulations were used to validate the DIRSIG plume model. For a given set of parameter values, the DIRSIG predicted temperature error was 0.724 K compared to a MODTRAN predicted temperature error of 0.737 K. The DIRSIG result is within 1.8 % of the MODTRAN result. For a typical LWIR camera sensitivity of 0.1 K, the difference between the DIRSIG and MODTRAN results is within the sensor noise.

These simulations may be used to predict the temperature errors that might be observed on a typical summer day at the Savannah River Site (SRS). A plume height of 5 meters and a plume temperature and dew point depression of 305 K and 2 K, respectively, were chosen as typical values. A blackbody temperature of 306 K was used. This would translate into a plume at about 90°F and 90% relative humidity. The temperature error under these conditions is approximately 0.75 K.

ACKNOWLEDGMENTS

The authors would like to extend a special thanks to Gail Anderson of the Air Force Research Laboratory, to the DIRS laboratory at the Center for Imaging Science at RIT, and to the Savannah River National Laboratory for their sponsorship under contract DE-AC09-96SR18500.

REFERENCES

1. P. Dash, F. M. Gottsche, F. S. Olesen, and H. Fischer, "Land surface temperature and emissivity estimation from passive sensor data: theory and practice - current trends," in *International Journal of Remote Sensing*, **23**(13), pp. 2563–2594, 2002.
2. W. L. Barnes and J. C. Price, "Calibration of a satellite infrared radiometer," in *Applied Optics*, **19**(13), pp. 2153–2161, 1980.
3. A. Berk, G. P. Anderson, L. S. Bernstein, P. K. Acharya, H. Dothe, M. W. Matthew, S. M. Adler-Golden, J. J. H. Chetwynd, S. C. Richtsmeier, B. Pukall, C. L. Allred, L. S. Jeong, and M. L. Hoke, "Modtran4 radiative transfer modeling for atmospheric correction," in *Optical Spectroscopic Techniques and Instrumentation for Atmospheric and Space Research III*, pp. 348–353, SPIE Vol. 3756, (Denver, Colorado), 1999.
4. "Nonconventional Exploitation Factors (NEF) Modeling," Tech. Rep. v9.5, April 2005.
5. E. Hecht, *Optics*, Addison-Wesley Publishing Company, Reading, Massachusetts, second ed., 1990.
6. J. R. Schott, *Remote Sensing: The Image Chain Approach*, Oxford University Press, New York, NY, 1997.
7. J. M. Wallace and P. V. Hobbs, *Atmospheric Science An Introductory Survey*, Academic Press, NY, 1977.
8. F. Sospedra, V. Caselles, and E. Valor, "Effective wavenumber for thermal infrared bands - application to landsat-tm," in *International Journal of Remote Sensing*, **19**(11), pp. 2105–2117, 1998.
9. K. Stamnes, S.-C. Tsay, W. Wiscombe, and K. Jayaweera, "Numerically stable algorithm for discrete-ordinate-method radiative transfer in multiple scattering and emitting layered media," in *Applied Optics*, pp. 2502–2509, No. 12, Vol. 27, June 1988.
10. G. Anderson, "Email correspondence." August 2007.
11. Digital Imaging and Remote Sensing Laboratory, Rochester, NY, *The DIRSIG User's Manual*, Feb 2006.
12. A. K. Blackadar, *Turbulence and Diffusion in the Atmosphere*, Springer-Verlag, 1997.